

The Development of Chiral Nematic Mesoporous Materials

Joel A. Kelly,^{‡,†} Michael Giese,^{‡,†} Kevin E. Shopsowitz,[‡] Wadood Y. Hamad,[§] and Mark J. MacLachlan^{*,‡}

[‡]Department of Chemistry, University of British Columbia, 2036 Main Mall, Vancouver, British Columbia V6T 1Z1, Canada

[§]FPIInnovations, 3800 Wesbrook Mall, Vancouver, British Columbia V6S 2L9, Canada

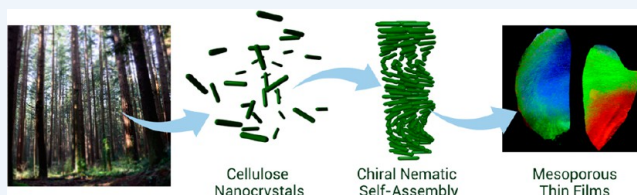
CONSPECTUS: Cellulose nanocrystals (CNCs) are obtained from the sulfuric acid-catalyzed hydrolysis of bulk cellulose. The nanocrystals have diameters of ~5–15 nm and lengths of ~100–300 nm (depending on the cellulose source and hydrolysis conditions). This lightweight material has mostly been investigated to reinforce composites and polymers because it has remarkable strength that rivals carbon nanotubes. But CNCs have an additional, less explored property: they organize into a *chiral nematic* (historically referred to as cholesteric) liquid crystal in water. When dried into a thin solid film, the CNCs retain the helicoidal chiral nematic order and assemble into a layered structure where the CNCs have aligned orientation within each layer, and their orientation rotates through the stack with a characteristic pitch (repeating distance). The cholesteric ordering can act as a 1-D photonic structure, selectively reflecting circularly polarized light that has a wavelength nearly matching the pitch.

During CNC self-assembly, it is possible to add sol–gel precursors, such as Si(OMe)₄, that undergo hydrolysis and condensation as the solvent evaporates, leading to a chiral nematic silica/CNC composite material. Calcination of the material in air destroys the cellulose template, leaving a high surface area mesoporous silica film that has pore diameters of ~3–10 nm. Importantly, the silica is brilliantly iridescent because the pores in its interior replicate the chiral nematic structure. These films may be useful as optical filters, reflectors, and membranes.

In this Account, we describe our recent research into mesoporous films with chiral nematic order. Taking advantage of the chiral nematic order and nanoscale of the CNC templates, new functional materials can be prepared. For example, heating the silica/CNC composites under an inert atmosphere followed by removal of the silica leaves highly ordered, mesoporous carbon films that can be used as supercapacitor electrodes. The composition of the mesoporous films can be varied by using assorted organosilica precursors. After removal of the cellulose by acid-catalyzed hydrolysis, highly porous, iridescent organosilica films are obtained. These materials are flexible and offer the ability to tune the chemical and mechanical properties through variation of the organic spacer.

Chiral nematic mesoporous silica and organosilica materials, obtainable as centimeter-scale freestanding films, are interesting hosts for nanomaterials. When noble metal nanoparticles are incorporated into the pores, they show strong circular dichroism signals associated with their surface plasmon resonances that arise from dipolar coupling of the particles within the chiral nematic host. Fluorescent conjugated polymers show induced circular dichroism spectra when encapsulated in the chiral nematic host. The porosity, film structure, and optical properties of these materials could enable their use in sensors.

We describe the development of chiral nematic mesoporous silica and organosilica, demonstrate different avenues of host–guest chemistry, and identify future directions that exploit the unique combination of properties present in these materials. The examples covered in this Account demonstrate that there is a rich diversity of composite materials accessible using CNC templating.



1. INTRODUCTION

Cellulose is the most abundant biopolymer on Earth and one of society's most important materials. Since antiquity, humans have exploited its renewability, vast availability, and unique material advantages (such as its exceptional mechanical properties^{1,2} and liquid crystalline order^{3,4}) for shelter, clothing, tools, paper, fuel, and many other purposes. In recent years, new forms of cellulose have attracted increasing interest for advanced materials applications.⁵ Many of these new applications are inspired by the elegant manner in which cellulose is deployed throughout the plant kingdom (Figure 1).

Microfibrillar cellulose is the major load-bearing component of plant cell walls. Depending on the orientation of these

microfibrils, the cell's mechanical properties can vary from stiff and strong to flexible and tough.⁶ The organization of cellulose microfibrils also plays a key role in plant morphogenesis, because they are wrapped in a helicoidal pattern around the cell that directs anisotropic cell expansion.^{7,8} Helical ordering of cellulosic materials in plant structures impacts not only cell growth and mechanical reinforcement; some plants exhibit brilliant iridescence through nanostructuring of cellulose in their flowers and leaves, which is thought to help attract

Received: October 9, 2013

Published: April 2, 2014

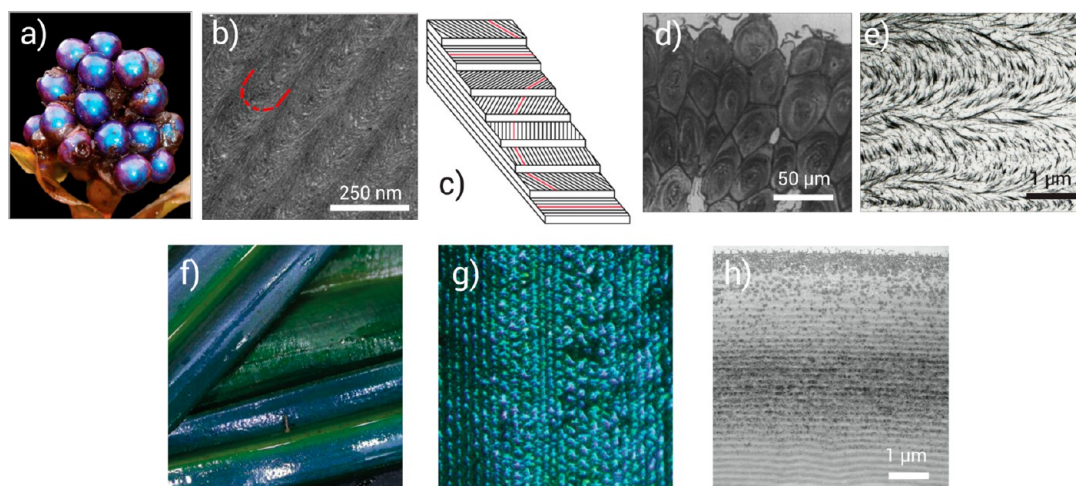


Figure 1. Examples of helicoidal organization of cellulose in plants. The blue iridescence of *Pollia condensata* fruit (a) is due to interference from cellulose-based helicoidal stacks (which can be observed using SEM, panel b).⁹ The helicoidal ordering of microfibrils can be visualized by a schematic showing the twist in the direction of orientation between layers (c). The epidermal cells of the seed coat of *Cydonia vulgaris* (d) exhibit large helicoidal spirals of cellulose microfibrils, which can be seen by TEM (panel e, adapted from ref 8 with permission from Elsevier). The blue-green iridescence of *Mapania caudata* leaves (f, g) is due to the helical ordering of cellulose in combination with biogenic silica (which can be observed using TEM, panel h).¹⁰

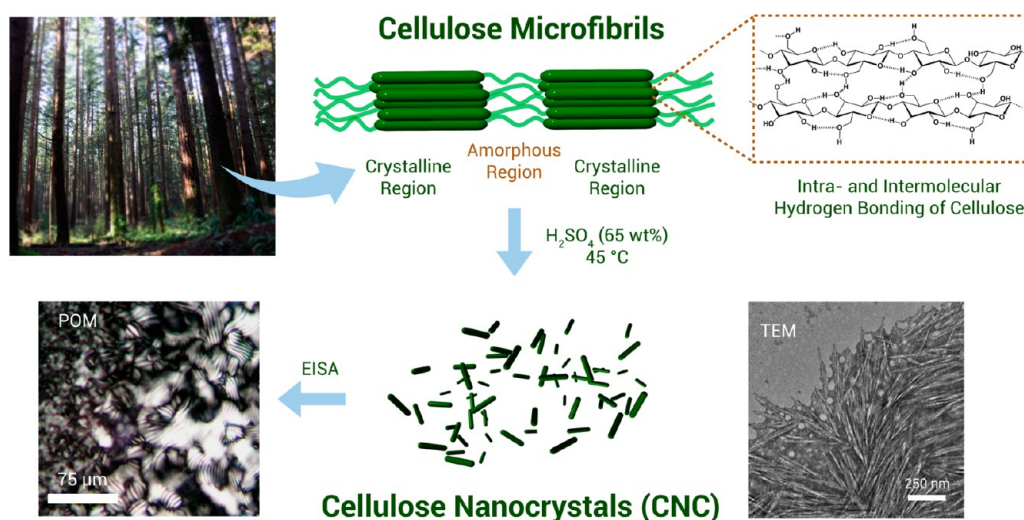


Figure 2. Acid hydrolysis of bulk cellulose material selectively removes hemicellulose and amorphous cellulose to produce cellulose nanocrystals (CNCs). The CNCs have a spindle-like morphology, which can be seen using TEM, and can self-assemble into chiral nematic liquid crystalline phases, which can be observed by POM as the formation of a fingerprint texture during evaporation.

pollinating species, increase seed dispersal, or possibly block UV radiation.^{9,10}

The organization of cellulose within plant cells depends on complex interactions between cellulose, hemicellulose, pectin, lignin, and structural proteins during morphogenesis.¹¹ However, the macromolecular structure of cellulose is a major contributor toward its unique material properties. Cellulose is a semicrystalline linear polymer of 1,4-linked D-glucose monomers. These polymers stack through extensive hydrogen bonding into highly crystalline nanoscale regions separated by amorphous domains arising from defects along the microfibril axis.⁴

In the early 1950s, researchers discovered that the amorphous regions of cellulose could be selectively removed through acid hydrolysis to isolate the rigid, rod-like crystallites, which are now termed cellulose nanocrystals (CNCs, Figure 2).¹² When sulfuric acid is employed, the CNCs have negatively

charged sulfate surface groups that enable them to form stable aqueous dispersions. The dimensions of CNCs are generally on the order of 5–15 nm in diameter and 100–300 nm in length, depending on the conditions of the hydrolysis and the cellulose feedstock (e.g., wood pulp, cotton, bacterial, tunicate). CNC has recently become the standard nomenclature following ISO protocol, but other terms have been used interchangeably in the literature, including nanocrystalline cellulose (NCC), cellulose nanowhiskers, cellulose microcrystals, and cellulose nanoparticles. Properties and development of CNCs and related materials have been extensively reviewed.^{5,13–17}

Lytotropic liquid crystalline behavior of cellulose crystallites has been known since the 1950s.³ In 1992, Revol and co-workers demonstrated that aqueous dispersions of CNCs could form chiral nematic phases at concentrations of ca. 3 wt %.¹⁸ In a chiral nematic liquid crystal, the rod-shaped mesogens have orientational order that twists with a characteristic repeat

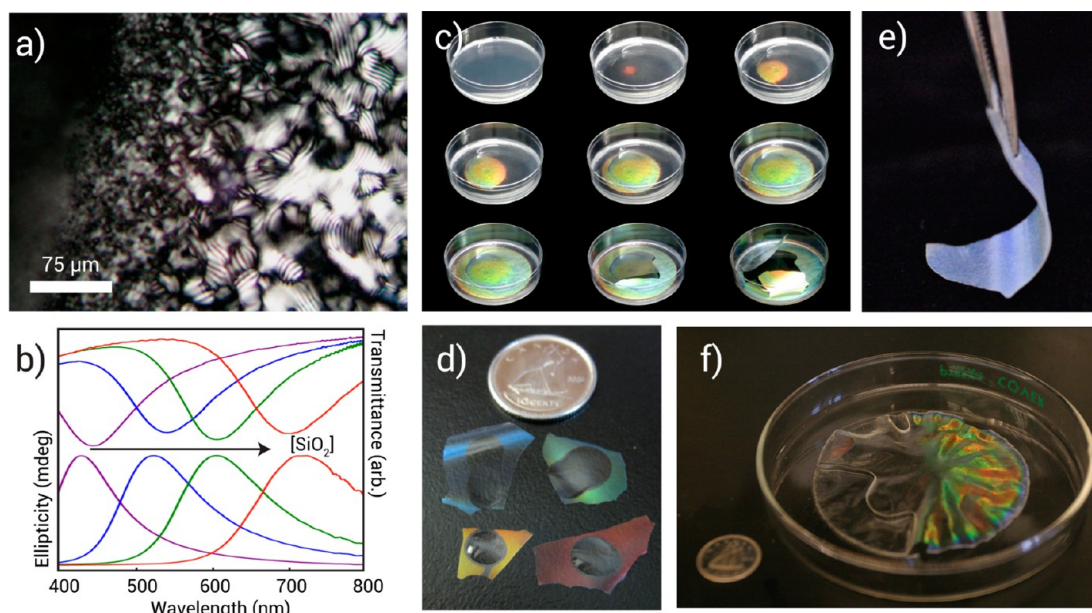


Figure 3. Self-assembly of CNCs with silica sol–gel precursors shows the characteristic formation of a fingerprint-like texture by POM (a) indicating the formation of a chiral nematic phase. Evaporating the mixture to dryness yields an iridescent composite (b, c) whose structural color depends on the silica loading. After removal of the CNCs through calcination or acid hydrolysis, mesoporous sol–gel derived films are obtained that retain their intense structural colors. The use of organosilica precursors yields films that are flexible and easily handled (e). Cracking observed during evaporation can be eliminated in the silica films by the addition of polyols such as glucose, leading to large, crack-free films (f). Adapted from refs 36, 37, 40, and 41 with permission from Macmillan Publishers Ltd., Wiley-VCH Verlag GmbH & Co, and the American Chemical Society.

distance termed the pitch. The formation of a lyotropic chiral nematic phase can be confirmed using polarized optical microscopy (POM) through the observation of fingerprint-like patterns as the water evaporates from the CNC dispersion. The helicoidal ordering of chiral nematic structures can produce brilliant color as observed in plants and certain animals (such as the chitinous exoskeleton of jewel beetles¹⁹), acting as a 1D photonic structure when the pitch is on the order of the wavelengths of visible light. In fact, the wavelength reflected depends on the pitch, the refractive index, and the viewing angle. Because the chiral nematic structure can be either left- or right-handed, the reflected light is always circularly polarized matching the handedness of the phase.

Several other cellulose derivatives such as hydroxypropylcellulose (HPC) and ethylcellulose also exhibit lyotropic chiral nematic behavior.^{20,21} However, CNC dispersions exhibit lyotropic chiral nematic behavior at much lower concentrations (e.g., 1–7 wt % compared with 50–75 wt % for HPC), have lower viscosities, and form over shorter time scales. This has attracted interest in the use of evaporation-induced self-assembly (EISA) of CNCs to prepare dried thin films with chiral nematic order for applications that exploit their brilliant iridescence such as security features or cosmetics. The reflected color can be tailored across the visible spectrum through several methods, for example, by adding salts to increase ionic strength (leading to a blue shift in color),²² ultrasonication of the dispersion before EISA (leading to a red shift),²³ or varying drying temperature (higher temperature leads to a blue shift).²⁴ Even though chiral nematic liquid crystals of some cellulose derivatives can exist as left- and right-handed structures,²¹ CNC dispersions appear to always form left-handed chiral nematic phases.

In this Account, we review our recent efforts to use CNCs to template new materials with chiral nematic structures. By carefully controlling the conditions and precursors employed,

diverse new materials with a unique combination of chiral photonic properties, high surface areas, and other novel properties can be prepared.

2. MESOPOROUS SILICA AND ORGANOSILICA FILMS WITH CHIRAL NEMATIC STRUCTURES

There is considerable current interest in materials that combine porosity with photonic structures as a method to tailor their resulting optical properties by infiltrating the pores with a suitable guest species.^{25,26} Examples of these materials include inverse opals,²⁷ mesoporous silicon prepared by electrochemical etching,²⁸ 1D Bragg stacks prepared by spin-coating alternating layers of metal oxide nanoparticles,²⁹ and opals prepared by self-assembly of mesoporous silica nanoparticles.³⁰ These materials have promise in a variety of areas such as sensors, lasing, and photovoltaics.

The high surface area, nanoscale dimensions, and lyotropic behavior of CNCs have attracted interest for their use as a template to prepare new kinds of porous materials. Examples of CNC-templated materials from other groups include porous TiO₂,³¹ shape-controlled TiO₂ cubes,³² and porous silica. Notably, Dujardin and co-workers prepared birefringent silica templated by CNCs under alkaline conditions but did not observe long-range chiral nematic ordering in the porous silica.³³ In a similar investigation, Thomas and Antonietti prepared chiral nematic silica/HPC composites, but the order was lost after cellulose removal.³⁴ In comparison, Che and co-workers have developed a family of chiral mesoporous materials templated using chiral surfactants,³⁵ but this chirality occurs on a different length scale than that of chiral nematic photonic structures.

In 2010, we discovered that alkoxysilane precursors such as tetramethoxysilane (TMOS) are compatible with CNC self-assembly for several reasons: (1) the isoelectric point of silica is near the pH of the as-prepared acidic CNC dispersions; (2)

hydrolysis of alkoxysilanes generates the corresponding alcohol, which does not perturb EISA; and (3) the slight acidity and high water ratio of the CNC dispersions suppress silica polymerization until the later stages of evaporation.^{36,37} Evaporating dispersions of CNCs and TMOS to dryness yields iridescent composite films whose reflected color can be varied from the UV across the visible and into the near IR spectral region with increasing TMOS content (Figure 3b,c). The tunable color is an excellent indication of intimately homogeneous CNC/silica composites; as the refractive indices of CNCs and silica are relatively close, the shift in the reflected wavelength is predominately due to an increase in the helical pitch. Circular dichroism (CD) spectroscopy shows that the reflection is exclusively left-handed circularly polarized light as expected from a CNC chiral nematic phase, with strong positive ellipticity matching the reflected wavelengths measured by UV-vis spectroscopy (Figure 3b). The self-assembly behavior occurs within a narrow pH range of ca. 2.5 to 4. Outside of this range, opaque, achiral composites are obtained due to the interplay between CNC self-assembly and silica polymerization.

Calcination of the composites at 540 °C removes the CNCs to give a mesoporous chiral nematic silica replica. Considerable contraction of the films occurs during heating (due to further condensation of the silica walls) leading to a decrease in the helical pitch. Also, cellulose is replaced with air ($n = 1.00$), leading to a net blue shift in the reflected color. Nitrogen adsorption measurements of the calcined silica films show high surface areas and pore volumes comparable with typical values reported for mesoporous silica. Pore distributions show peak pore diameters of ca. 3 nm with little distribution beyond 10 nm; this is consistent with templating from individual CNCs rather than aggregates.

XRD patterns confirm that the calcined silica is amorphous. Because the silica pore walls are locally isotropic, the strong iridescence and birefringence of the calcined films is entirely due to the anisotropic mesoscopic ordering induced by CNC self-assembly, a phenomenon known as form birefringence.³⁸ As a result, the porous silica films become transparent to the eye when their pores are filled with a liquid such as water whose refractive index is a close match to silica, regaining their iridescence as the liquid evaporates (Figure 3d). A residual signal can still be observed using CD spectroscopy from the optically transparent films because the refractive indices are not perfectly matched; this signal gradually decreases and red shifts as the refractive index inside the pores increases and becomes closer to that of silica.³⁷ This could form the basis for a chiral photonic sensor since the sensitivity we observe is comparable to other state-of-the-art refractive index-based sensors.

CNC EISA is also compatible with other sol-gel precursors related to the tetraalkoxysilanes. Periodic mesoporous organosilicas (PMOs), first developed in the late 1990s, use sol-gel silica precursors with bridging organic groups of the type $(RO)_3Si-R'-Si(OR)_3$ (R' is most commonly a small organic chain such as methylene or ethylene) as an approach to controllably incorporate organic groups at high levels into the pore walls of ordered mesoporous materials.³⁹ The sol-gel process for these precursors is similar to using TMOS, and EISA with CNCs produces analogous iridescent composites.⁴⁰ However, the bridging organic group cannot withstand calcination to remove CNCs, so we developed an alternative removal method. Treating ethylene-bridged organosilica composites with hot 6 M sulfuric acid followed by rinsing

with piranha solution completely removes the CNCs without damaging the organosilica pore walls, which we confirmed by solid-state NMR spectroscopy.⁴⁰ In comparison with brittle silica films produced from TMOS, films prepared with bridging ethylene groups have significantly improved mechanical properties; they are flexible and can be easily bent, picked up, and handled (Figure 3e).

The surface areas of the mesoporous organosilica films are high, consistent with complete template removal. However, the films have higher pore volumes than calcined silica samples and pore diameters that more closely reflect the average CNC diameters measured by electron microscopy. Similar pore diameters are obtained with chiral nematic silica samples where the CNC was removed by acid extraction, suggesting that the acid extraction process does not induce the significant contraction observed for calcination and thus indirectly presents a method to control the pore diameter and volume. We have also prepared organosilica films with a bridging 1,4-phenylene precursor and found that the CNCs could be effectively removed with hot HCl followed by a silver-activated hydrogen peroxide wash.⁴²

High-resolution electron microscopy of these sol-gel derived materials reveals their helically twisting structures arising from the chiral nematic CNC ordering. When the films are fractured normal to their surface, layers with a pitch on the order of hundreds of nanometers can be observed using scanning electron microscopy (SEM). In some areas, fingerprint-like defects appear that are similar to the ordering observed during the early stages of EISA by POM. The use of helium ion microscopy (HIM) allows these insulating samples to be imaged directly without sputter coating and facilitates the acquisition of very high resolution images (Figure 4).⁴² At these magnifications, ethylene-bridged films appear as a porous, woven network of whisker-like organosilica. The average pore size measured by HIM is 8.4 ± 2.1 nm, in good agreement with gas adsorption measurements. In all of these materials, the observed twisting chiral nematic helices are left-handed, replicating the handedness of the parent CNC liquid crystalline phases.

A significant limitation to using these materials in applications that require large, homogeneous films is that the films tend to crack during the last stages of EISA into centimeter-sized pieces. As observed in other mesoporous materials, this is due to the generation of significant capillary pressure gradients during evaporation. To address this issue, we found that cracking can be eliminated in the mesoporous silica films by the addition of simple polyols (e.g., glucose) to the CNC dispersion before EISA, which alters the sol-gel curing kinetics.⁴¹ This simple modification does not significantly affect the films' optical properties or mesoporosity and allows upward of ca. 15 cm diameter crack-free silica films to be produced by calcination (Figure 3f). However, our attempts to prepare crack-free organosilica films were unsuccessful, because it appears the perturbation of the sol-gel equilibria does not provide sufficient condensation to survive the acid extraction process. It is interesting to note that both enantiomers of glucose gave films with left-handed chiral nematic ordering, demonstrating that the self-assembly is likely not driven by hydrogen bonding on the surface of the CNCs.

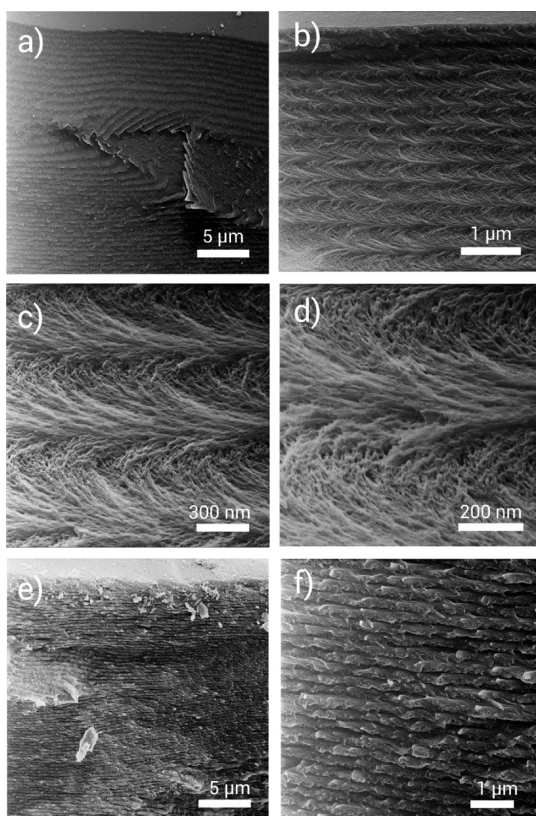


Figure 4. Helium ion microscopy of chiral nematic mesoporous (a–d) ethylene-bridged organosilica and (e, f) silica at varying magnification. Adapted from ref 42 with permission from the Royal Society of Chemistry.

3. HARD TEMPLATING OF MESOPOROUS CHIRAL NEMATIC MATERIALS

Hard templating using preformed mesoporous materials (also termed “nanocasting”) has emerged as a versatile technique to prepare materials that cannot be accessed through conventional lyotropic template synthesis (e.g., due to hydrolytic instability of precursors).⁴³ In this approach, successive loadings of the precursor are infiltrated into a stable mesoporous support, often followed by calcination to build up an interconnected network of the desired product. Many kinds of ordered mesoporous materials (e.g., carbon, metal oxides, and polymers) can be prepared through hard templating. Notably, mesoscopically ordered titania prepared via hard templating has attracted intense interest for its photocatalytic activity, incorporation into dye-sensitized solar cells, and high refractive index ($n \approx 2.5$) for photonic applications.⁴⁴

We prepared chiral nematic titania films through repeated loading of a peptized TiCl_4 solution (a precursor that instantaneously gels aqueous CNC dispersions) into mesoporous chiral nematic silica films followed by annealing.⁴⁵ After four cycles of loading, the silica–titania composite was calcined at 600 °C, and the silica support was removed by etching in 2 M NaOH to yield freestanding, mesoporous titania films whose iridescence was exclusively left-handed circularly polarized (Figure 5a). The hard templating could be carried out using silica films prepared through either calcination or acid extraction to give mesoporous titania with varying pore diameters, pore volumes, and surface areas.⁴⁵ While both types of films reproduced iridescence characteristic of chiral

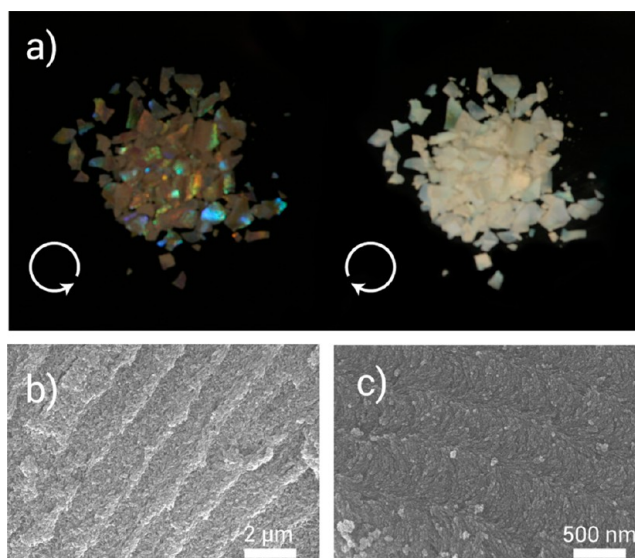


Figure 5. Chiral nematic mesoporous titania thin films appear iridescent through a left-handed circularly polarized filter and opaque white through a right-handed filter (a), illustrating the selective reflection in these materials. SEM of the thin films (b, c) confirms the replication of the helical structure, with globules likely introduced by titania crystallization. Adapted from ref 45 with permission from Wiley-VCH Verlag GmbH & Co.

nematic order in the resulting titania, samples prepared using acid-extracted silica had larger dimensions and qualitatively more intense iridescence, suggesting that the larger mesopores achieved through acid extraction allowed for more effective diffusion of the titania precursor.

SEM of the hard-templated titania confirmed replication of the helical chiral nematic structure with a globular morphology evident at higher magnification likely due to crystallization of the titania (Figure 5b,c). XRD patterns of these titania films show they are composed of nanocrystalline anatase, rather than the thermodynamically favored rutile phase, due to confinement inside the mesopores during crystallization.⁴⁵ The successful replication of chiral nematic order in titania through hard templating confirms the interconnected nature of the pore network in these CNC-derived materials and is proof-of-concept for a general strategy to prepare other chiral nematic materials.

4. MESOPOROUS CARBON FILMS DERIVED FROM CNC/SIO₂ COMPOSITES

The development of porous carbon materials with high specific surface areas, large pore volumes, and large adsorption capacities has stoked interest in applications including electrode materials, sorbents in separation processes, and catalyst supports.⁴⁶ In particular, their use as high surface area electrodes in electrical double-layer supercapacitors has led to devices with promising high specific capacitance values.⁴⁷ In all of these applications, two often-encountered drawbacks of porous carbon materials are slow mass transport properties due to significant microporosity and elaborate, time-consuming, or expensive preparative methods to produce large area electrodes that could be impractical for use at commercial scale.

The CNC/silica composites used to prepare iridescent, mesoporous silica films can alternatively be used to prepare freestanding mesoporous carbon films, simply by pyrolysis

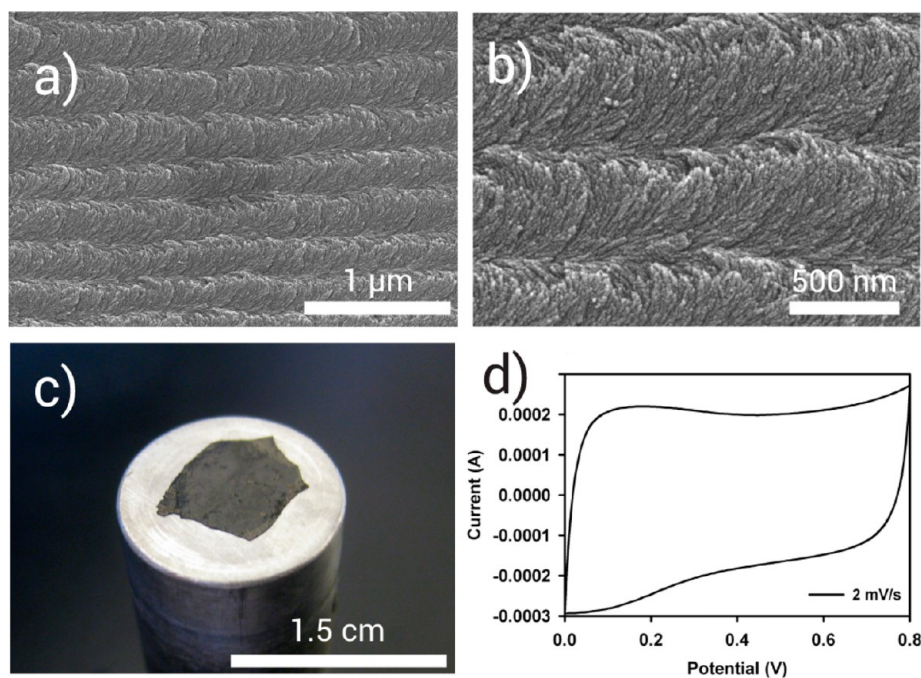


Figure 6. Chiral nematic mesoporous carbon films prepared by pyrolysis of CNC/silica composites exhibit helical twisting morphologies by SEM (a, b). The freestanding films can be used directly without any binders as electrodes in electrical double-layer supercapacitors (c) and display near-ideal capacitor behavior (d), with specific capacitances comparable to other state-of-the-art carbon-based supercapacitors. Adapted from ref 48 with permission from Wiley-VCH Verlag GmbH & Co.

under nitrogen at 900 °C (instead of calcining under air) followed by etching of the silica.⁴⁸ The resulting glossy black films are obtained in about 30% yield as amorphous carbon and are semiconducting at room temperature. The porosity of the films varies with the silica loading, ranging from largely microporous for pure CNC-derived samples to completely mesoporous for 65 wt % CNC samples; the surface area and pore volume of the mesoporous samples is comparable to carbon materials prepared by hard templating. SEM of these samples echoes the long-range ordering observed for their corresponding silica samples, with helical twisting indicative of chiral nematic self-assembly (Figure 6a,b).

Owing to their freestanding nature, the mesoporous carbon films can be used directly as supercapacitor electrodes without a binding agent typically needed for other mesoporous carbon electrodes (Figure 6c). In a symmetrical capacitor with aqueous sulfuric acid as the electrolyte, the mesoporous carbon films display near-ideal capacitor behavior (Figure 6d). Their specific capacitance is 170 F g⁻¹ at a current load of 230 mA g⁻¹, with performance decreasing at higher power loads.⁴⁸ These results are comparable to values reported for mesoporous carbons prepared through hard templating with various mesoporous silicates. The nanostructured features in the chiral nematic mesoporous carbon films may lead them to applications as novel catalyst supports or gas storage membranes.

5. MESOPOROUS SCAFFOLDS FOR CHIRAL OPTICAL EFFECTS

The high surface area and mesoporosity of these CNC-templated sol-gel-derived materials facilitates their use as scaffolds for guest species exhibiting novel chiral optical properties through chiral nematic organization. In this section, we highlight some of the recent advances we have made in preparing guest species inside the CNC-templated materials,

which could be appealing for applications such as catalysis, sensing, and optoelectronics.

Noble metal nanoparticles (NPs) are attractive for developing biochemical sensors that generate a change in the surface plasmon resonance (SPR) upon binding of a desired analyte. Chiral assemblies of NPs are especially promising candidates because the circular dichroism of the SPR gives rise to an excellent sensitivity and detection limit.^{49,50} In 2011, our group demonstrated the first examples of chiral metal nanoparticle assemblies without the use of a chiral ligand or biotemplate.⁵¹ Silver NPs were prepared by *in situ* reduction of AgNO₃ inside the pores of calcined chiral nematic mesoporous silica. The materials showed a strong CD signal for the SPR peak that varied with the helical pitch (Figure 7b). Detailed CD spectroscopic investigations and control experiments proved that the observed chirality originates from the helical pitch of the mesoporous material rather than from the molecular chirality of the CNC imprinting in the silica. Recently, we used a new one-pot synthesis method to make chiral nematic mesoporous silica films decorated with assemblies of gold, silver, and platinum metal NPs.⁵² In this method, compatible precursors of metal NPs are coassembled with the CNC silica composites, leading to the corresponding mesoporous chiral nematic silica films decorated with metal NPs upon calcination (Figure 7a). CD spectroscopy of the silver and gold NP hybrid materials show that the metal NPs have induced CD spectra of their SPR bands attributed to their chiral organization. We observed significant changes in both CD and UV-vis spectra upon changes in their environment (different solvents or the introduction of surface-bound ligands). Considering the importance of the SPR of metal NPs in biochemical sensing, these new chiral nematic NP composite materials open up new directions in chemical sensing applications based on the CD

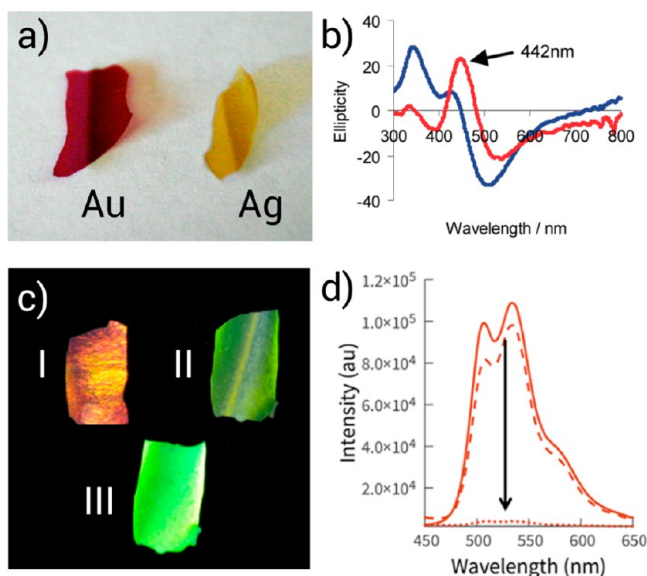


Figure 7. Photographs and characterization of new hybrid materials templated by CNCs. (a) Silica films doped with gold and silver NPs showing characteristic colors arising from the plasmon resonance of the NPs.⁵² CD spectra clearly demonstrate the induction of chirality to the plasmon resonance by the chiral nematic surrounding (b).⁵¹ (c) Photographs showing chiral nematic organosilica films before (I) and after doping with PPV (II), as well as fluorescence from PPV composites under UV illumination (III).⁵³ (d) Fluorescence quenching of the PPV composites by diluted solutions of TNT demonstrating their potential use in sensing. Adapted from refs 51–53.

response of the chiral assemblies of NPs in chiral nematic mesoporous hosts.

Chiral nematic ordering in conjugated polymers (for example, by polymerizing in a chiral nematic solvent) can give rise to novel magnetic, electronic, and optical properties.⁵⁴ The combination of mesoporosity and chiral nematic order in the present materials facilitates the convenient preparation of conjugated polymers inside the pores. We recently formed poly(phenylene vinylene) (PPV) within chiral nematic mesoporous organosilica.⁵³ This was achieved by surface-induced polymerization of xylene bis(tetrahydrothiophenium bromide) in chiral nematic mesoporous organosilica films, yielding bright yellow, iridescent PPV–organosilica composites (Figure 7c) with chiral long-range alignment of the PPV inside the mesoporous host. The polymer was accessible to analytes and underwent fluorescence quenching when exposed to electron-deficient aromatic guests (e.g., TNT), Figure 7d. This is a new approach to the organization of conjugated polymers within a chiral host and might have a significant impact on the development of novel devices based on the anisotropic ordering of these hybrid materials.

Reversible control of the optical properties of photonic materials is a major goal for the development of devices such as reflective displays, filters, or sensors.⁵⁵ The optical properties of photonic materials can potentially be varied by addressing either their periodicity or their refractive index contrast. Embedding responsive guests within the channels of a chiral nematic mesoporous host could allow for stimuli-induced changes in refractive index and thus dynamic modification of the optical properties of the composite. In this context, thermotropic liquid crystals (LCs) are interesting guests to incorporate since they show large changes in their refractive

indices and molecular alignment in response to temperature changes and therefore offer a thermal switch to control the reflection in chiral nematic mesoporous organosilica films. In 2013, we infiltrated octyl-functionalized chiral nematic organosilica films with 4-cyano-4'-octylbiphenyl (8CB), a well-studied thermotropic liquid crystal.⁵⁶ The films are strongly iridescent at room temperature; upon heating, they undergo a rapid change to colorless near the nematic to isotropic transition temperature for 8CB at ~ 40 °C. The changes in optical properties are best illustrated with the complete loss of the reflection signal in the UV–vis spectra for the LC-loaded films (Figure 8). Correlation of the observed color change with the

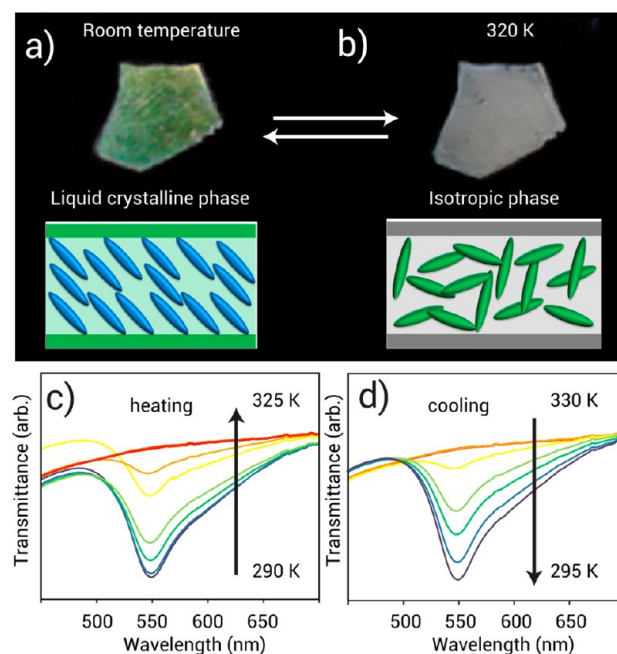


Figure 8. Infiltration of chiral nematic organosilica films with the liquid crystal 8CB gives composite materials that reversibly change their color from green (a) to transparent (b) upon heating from the liquid crystalline phase to the isotropic phase. The change in color and its reversibility is quantified by UV–vis studies showing the decrease of the photonic signal upon heating the sample to 50 °C (c) and the return of the photonic signal upon cooling to room temperature (d). Adapted from ref 56.

alignment of the 8CB molecules was investigated by variable-temperature solid-state NMR spectroscopy of a ¹⁵N-labeled 8CB derivative revealing the alignment of the rod-shaped guests within the pores while in the liquid-crystalline state.⁵⁶ Upon reaching the isotropic phase, the solid-state NMR spectra prove the liquid-like nature of the mesogen within the channels. This approach to thermoresponsive materials with tunable properties may be interesting for the development of switchable components in displays or sensors. Further investigations on related composites are currently in progress and might give additional insight into the molecular alignment and confinement within the channels of a chiral nematic mesoporous host.

6. OUTLOOK AND CONCLUSIONS

The potential to emulate the chiral nematic organization of cellulose in plant cell walls through CNC self-assembly has opened the path to multiple new research directions. By use of liquid crystal templating, the chiral nematic organization of CNCs can successfully be transferred to solid-state composite

materials based on silica and organosilica. The resulting iridescent CNC/(organo)silica composites can be transformed into a range of new materials, including highly porous semiconducting carbon films with chiral nematic order that function well as supercapacitor electrodes. Alternatively, the CNC template can be removed from the CNC/(organo)silica composites to leave (organo)silica films that are iridescent, mesoporous, and flexible. These films, which can be prepared on a large scale, are promising as reflectors, sensors, membranes, and sorbents. Moreover, encapsulation of guests within the channels gives opportunities to produce new functional, responsive materials and to transfer chiral nematic order to other solid-state compositions.

These chiral nematic solid-state materials have considerable potential for creating new devices and catalysts. Their availability as large, freestanding films is useful for many applications, including windows and filters. We are continuing to develop new templated materials with chiral nematic order that can offer additional flexibility or new materials properties.^{57,58} Also, the successful encapsulation of other functional guests, such as quantum dots, has recently been investigated.⁵⁹

AUTHOR INFORMATION

Author Contributions

†J.A.K. and M.G. contributed equally to this work.

Notes

The authors declare no competing financial interest.

Biographies

Joel Kelly received his B.Sc. degree from King's University College and his Ph.D. from the University of Alberta in 2011. In 2011, he joined the MacLachlan lab as an NSERC Postdoctoral fellow.

Michael Giese studied chemistry at the RWTH Aachen University where he received his Ph.D. in 2011. After graduation, he joined the group of Prof. Mark MacLachlan as a DAAD Postdoctoral Fellow working on new functional materials templated by cellulose nanocrystals.

Kevin Shopsowitz completed his B.Sc. degree in Biochemistry at McGill University and his Ph.D. degree at UBC under the guidance of Prof. MacLachlan. He received the Award for Graduate Research in Inorganic Chemistry from the Chemical Institute of Canada (2012) and is now an NSERC Postdoctoral Fellow in Chemical Engineering at MIT.

Wadood Hamad holds a Ph.D. in polymer physics and micro-mechanics from McGill. He is Principal Scientist at FPIInnovations whose work over the past decade has focused on scaling up CNC production and exploring new advanced applications.

Mark MacLachlan has been at UBC since 2001, where he is now Professor. He is the 2012 recipient of the NSERC E.W.R. Steacie Memorial Fellowship and 2013 Rutherford Medal of the Royal Society of Canada.

REFERENCES

(1) Sakurada, I.; Nukushina, Y.; Ito, T. Experimental Determination of the Elastic Modulus of Crystalline Regions in Oriented Polymers. *J. Polym. Sci.* **1962**, *57*, 651–660.
(2) Takayanagi, M.; Uemura, S.; Minami, S. Application of Equivalent Model Method to Dynamic Rheo-Optical Properties of Crystalline Polymer. *J. Polym. Sci., Part C: Polym. Symp.* **1964**, *5*, 113–122.

(3) Marchessault, R. H.; Morehead, F. F.; Walter, N. M. Liquid Crystal Systems From Fibrillar Polysaccharides. *Nature* **1959**, *184*, 632–633.
(4) Frey-Wyssling, A.; Muhlethaler, K. *Ultrastructural Plant Cytology*; Elsevier Publishing Company, New York, 1965; pp 34–40.
(5) Klemm, D.; Kramer, F.; Moritz, S.; Lindström, T.; Ankerfors, M.; Gray, D.; Dorris, A. Nanocelluloses: A New Family of Nature-Based Materials. *Angew. Chem., Int. Ed.* **2011**, *50*, 5438–5466.
(6) Eder, M.; Jungnickl, K.; Burgert, I. A Close-Up View of Wood Structure and Properties across a Growth Ring of Norway Spruce (*Picea abies* [L.] Karst). *Trees* **2009**, *23*, 79–84.
(7) Gillmor, C. S.; Poindexter, P.; Lorieau, J.; Palcic, M. M.; Somerville, C. Alpha-Glucosidase I Is Required for Cellulose Biosynthesis and Morphogenesis in *Arabidopsis*. *J. Cell Biol.* **2002**, *156*, 1003–1013.
(8) Abeyssekera, R. M.; Willison, J. H. M. A Spiral Helicoid in a Plant Cell Wall. *Cell Biol. Int.* **1987**, *11*, 75–79.
(9) Vignolini, S.; Moyroud, E.; Glover, B. J.; Steiner, U. Analysing Photonic Structures in Plants. *J. R. Soc. Interface* **2013**, *10*, No. 20130394.
(10) Strout, G.; Russell, S. D.; Pulsifer, D. P.; Erten, S.; Lakhtakia, A.; Lee, D. W. Silica Nanoparticles Aid in Structural Leaf Coloration in the Malaysian Tropical Rainforest Understorey Herb *Mapania Caudata*. *Ann. Bot.* **2013**, No. mct172.
(11) Teeri, T. T.; Brumer, H.; Daniel, G.; Gatenholm, P. Biomimetic Engineering of Cellulose-Based Materials. *Trends Biotechnol.* **2007**, *25*, 299–306.
(12) Rånby, B. G. Aqueous Colloidal Solutions of Cellulose Micelles. *Acta Chem. Scand.* **1949**, *3*, 649–650.
(13) Habibi, Y.; Lucia, L. A.; Rojas, O. J. Cellulose Nanocrystals: Chemistry, Self-Assembly, and Applications. *Chem. Rev.* **2010**, *110*, 3479–3500.
(14) Hamad, W. Y. Development and Properties of Nanocrystalline Cellulose. In *Sustainable Production of Fuels, Chemicals, and Fibers from Forest Biomass*; Zhu, J.; Zhang, X.; Pan, X., Eds.; ACS Symposium Series 1067; American Chemical Society: Washington, DC, 2011; pp 301–321.
(15) Peng, B. L.; Dhar, N.; Liu, H. L.; Tam, K. C. Chemistry and Applications of Nanocrystalline Cellulose and Its Derivatives: A Nanotechnology Perspective. *Can. J. Chem. Eng.* **2011**, *89*, 1191–1206.
(16) Siqueira, G.; Bras, J.; Dufresne, A. Cellulosic Bionanocomposites: A Review of Preparation, Properties and Applications. *Polymers* **2010**, *2*, 728–765.
(17) Moon, R. J.; Martini, A.; Nairn, J.; Simonsen, J.; Youngblood, J. Cellulose Nanomaterials Review: Structure, Properties and Nanocomposites. *Chem. Soc. Rev.* **2011**, *40*, 3941–3994.
(18) Revol, J. F.; Bradford, H.; Giasson, J.; Marchessault, R. H.; Gray, D. G. Helicoidal Self-Ordering of Cellulose Microfibrils in Aqueous Suspension. *Int. J. Biol. Macromol.* **1992**, *14*, 170–172.
(19) Sharma, V.; Crne, M.; Park, J. O.; Srinivasarao, M. Structural Origin of Circularly Polarized Iridescence in Jeweled Beetles. *Science* **2009**, *325*, 449–451.
(20) Kamide, K. *Cellulose and Cellulose Derivatives*, 1st ed.; Elsevier B.V.: Amsterdam, 2005.
(21) Harkness, B. R.; Gray, D. G. Left- and Right-Handed Chiral Nematic Mesophase of (Trityl)(Alkyl)Cellulose Derivatives. *Can. J. Chem.* **1990**, *68*, 1135–1139.
(22) Dong, X. M.; Gray, D. G. Effect of Counterions on Ordered Phase Formation in Suspensions of Charged Rodlike Cellulose Crystallites. *Langmuir* **1997**, *13*, 2404–2409.
(23) Beck, S.; Bouchard, J.; Berry, R. Controlling the Reflection Wavelength of Iridescent Solid Films of Nanocrystalline Cellulose. *Biomacromolecules* **2011**, *12*, 167–172.
(24) Pan, J.; Hamad, W.; Straus, S. K. Parameters Affecting the Chiral Nematic Phase of Nanocrystalline Cellulose Films. *Macromolecules* **2010**, *43*, 3851–3858.
(25) von Freymann, G.; Kitaev, V.; Lotsch, B. V.; Ozin, G. A. Bottom-Up Assembly of Photonic Crystals. *Chem. Soc. Rev.* **2013**, *42*, 2528–2554.

- (26) Calvo, M. E.; Colodrero, S.; Hidalgo, N.; Lozano, G.; López-López, C.; Sánchez-Sobrado, O.; Míguez, H. Porous One Dimensional Photonic Crystals: Novel Multifunctional Materials for Environmental and Energy Applications. *Energy Environ. Sci.* **2011**, *4*, 4800–4812.
- (27) Petkovich, N. D.; Stein, A. Controlling Macro- and Mesopores with Hierarchical Porosity through Combined Hard and Soft Templating. *Chem. Soc. Rev.* **2013**, *42*, 3721–3739.
- (28) Lin, V. S.; Motesharei, K.; Dancil, K. P.; Sailor, M. J.; Ghadiri, M. R. A Porous Silicon-Based Optical Interferometric Biosensor. *Science* **1997**, *278*, 840–843.
- (29) Choi, S. Y.; Mamak, M.; von Freymann, G.; Chopra, N.; Ozin, G. A. Mesoporous Bragg Stack Color Tunable Sensors. *Nano Lett.* **2006**, *6*, 2456–2461.
- (30) Yamada, Y.; Nakamura, T.; Ishi, M.; Yano, K. Reversible Control of Light Reflection of a Colloidal Crystal Film Fabricated from Monodisperse Mesoporous Silica Spheres. *Langmuir* **2006**, *22*, 2444–2446.
- (31) Shin, Y.; Exarhos, G. J. Template Synthesis of Porous Titania Using Cellulose Nanocrystals. *Mater. Lett.* **2007**, *61*, 2594–2597.
- (32) Zhou, Y.; Ding, E.-Y.; Li, W.-D. Synthesis of TiO₂ Nanocubes Induced by Cellulose Nanocrystal (CNC) at Low Temperature. *Mater. Lett.* **2007**, *61*, 5050–5052.
- (33) Dujardin, E.; Blaseby, M.; Mann, S. Synthesis of Mesoporous Silica by Sol–Gel Mineralisation of Cellulose Nanorod Nematic Suspensions. *J. Mater. Chem.* **2003**, *13*, 696–699.
- (34) Thomas, A.; Antonietti, M. Silica Nanocasting of Simple Cellulose Derivatives: Towards Chiral Pore Systems with Long-Range Order and Chiral Optical Coatings. *Adv. Funct. Mater.* **2003**, *13*, 763–766.
- (35) Qiu, H.; Che, S. Chiral Mesoporous Silica: Chiral Construction and Imprinting via Cooperative Self-Assembly of Amphiphiles and Silica Precursors. *Chem. Soc. Rev.* **2011**, *40*, 1259–1268.
- (36) Shopsowitz, K. E.; Qi, H.; Hamad, W. Y.; MacLachlan, M. J. Free-Standing Mesoporous Silica Films with Tunable Chiral Nematic Structures. *Nature* **2010**, *468*, 422–425.
- (37) Shopsowitz, K. E.; Kelly, J. A.; Hamad, W. Y.; MacLachlan, M. J. Biopolymer Templated Glass with a Twist: Controlling the Chirality, Porosity, and Photonic Properties of Silica with Cellulose Nanocrystals. *Adv. Funct. Mater.* **2014**, *24*, 327–338.
- (38) Bragg, W. L.; Pippard, A. B. The Form Birefringence of Macromolecules. *Acta Crystallogr.* **1953**, *6*, 865–867.
- (39) MacLachlan, M. J.; Asefa, T.; Ozin, G. A. Writing on the Wall with a New Synthetic Quill. *Chem.—Eur. J.* **2000**, *6*, 2507–2511.
- (40) Shopsowitz, K. E.; Hamad, W. Y.; MacLachlan, M. J. Flexible and Iridescent Chiral Nematic Mesoporous Organosilica Films. *J. Am. Chem. Soc.* **2012**, *134*, 867–870.
- (41) Kelly, J. A.; Yu, M.; Hamad, W. Y.; MacLachlan, M. J. Large, Crack-Free Freestanding Films with Chiral Nematic Structures. *Adv. Opt. Mater.* **2013**, *1*, 295–299.
- (42) Terpstra, A. S.; Shopsowitz, K. E.; Gregory, C. F.; Manning, A. P.; Michal, C. A.; Hamad, W. Y.; Yang, J.; MacLachlan, M. J. Helium Ion Microscopy: A New Tool for Imaging Novel Mesoporous Silica and Organosilica Materials. *Chem. Commun.* **2013**, *49*, 1645–1647.
- (43) Lu, A. H.; Zhao, D.; Wan, Y. *Nanocasting: A Versatile Strategy for Creating Nanostructured Porous Materials*; The Royal Society of Chemistry: Cambridge, U.K., 2009.
- (44) Zhang, R.; Elzatahry, A. A.; Al-Deyab, S. S.; Zhao, D. Mesoporous Titania: From Synthesis to Application. *Nano Today* **2012**, *7*, 344–366.
- (45) Shopsowitz, K. E.; Stahl, A.; Hamad, W. Y.; MacLachlan, M. J. Hard Templating of Nanocrystalline Titanium Dioxide with Chiral Nematic Ordering. *Angew. Chem., Int. Ed.* **2012**, *51*, 6886–6890.
- (46) Lee, J.; Kim, J.; Hyeon, T. Recent Progress in the Synthesis of Porous Carbon Materials. *Adv. Mater.* **2006**, *18*, 2073–2094.
- (47) Zhang, L. L.; Zhao, X. S. Carbon-Based Materials as Supercapacitor Electrodes. *Chem. Soc. Rev.* **2009**, *38*, 2520–2531.
- (48) Shopsowitz, K. E.; Hamad, W. Y.; MacLachlan, M. J. Chiral Nematic Mesoporous Carbon Derived from Nanocrystalline Cellulose. *Angew. Chem., Int. Ed.* **2011**, *50*, 10991–10995.
- (49) Govorov, A. O.; Gun'ko, Y. K.; Slocik, J. M.; Gérard, V. A.; Fan, Z.; Naik, R. R. Chiral Nanoparticle Assemblies: Circular Dichroism, Plasmonic Interactions, and Exciton Effects. *J. Mater. Chem.* **2011**, *21*, 16806–16818.
- (50) Gautier, C.; Bürgi, T. Chiral Gold Nanoparticles. *ChemPhysChem* **2009**, *10*, 483–492.
- (51) Qi, H.; Shopsowitz, K. E.; Hamad, W. Y.; MacLachlan, M. J. Chiral Nematic Assemblies of Silver Nanoparticles in Mesoporous Silica Thin Films. *J. Am. Chem. Soc.* **2011**, *133*, 3728–3731.
- (52) Kelly, J. A.; Shopsowitz, K. E.; Ahn, J. M.; Hamad, W. Y.; MacLachlan, M. J. Chiral Nematic Stained Glass: Controlling the Optical Properties of Nanocrystalline Cellulose-Templated Materials. *Langmuir* **2012**, *28*, 17256–17262.
- (53) Mehr, S. H. M.; Giese, M.; Qi, H.; Shopsowitz, K. E.; Hamad, W. Y.; MacLachlan, M. J. Novel PPV/Mesoporous Organosilica Composites: Influence of the Host Chirality on a Conjugated Polymer Guest. *Langmuir* **2013**, *29*, 12579–12584.
- (54) Akagi, K.; Piao, G.; Kaneko, S.; Sakamaki, K.; Shirakawa, H.; Kyotani, M. Helical Polyacetylene Synthesized with a Chiral Nematic Reaction Field. *Science* **1998**, *282*, 1683–1686.
- (55) Ruda, H.; Matsuura, N. Nano-Engineered Tunable Photonic Crystals in the Near-IR and Visible Electromagnetic Spectrum. in *Springer Handbook of Electronic and Photonic Materials*; Kasap, S., Capper, P., Eds.; Springer: Boston, MA, 2007; pp 997–1019.
- (56) Giese, M.; De Witt, J. C.; Shopsowitz, K. E.; Manning, A. P.; Dong, R. Y.; Michal, C. A.; Hamad, W. Y.; MacLachlan, M. J. Thermal Switching of the Reflection in Chiral Nematic Mesoporous Organosilica Films Infiltrated with Liquid Crystals. *ACS Appl. Mater. Interfaces* **2013**, *5*, 6854–6859.
- (57) Kelly, J. A.; Shukaliak, A. M.; Cheung, C. C. Y.; Shopsowitz, K. E.; Hamad, W. Y.; MacLachlan, M. J. Responsive Photonic Hydrogels Based on Nanocrystalline Cellulose. *Angew. Chem., Int. Ed.* **2013**, *52*, 8912–8916.
- (58) Khan, M. K.; Giese, M.; Yu, M.; Kelly, J. A.; Hamad, W. Y.; MacLachlan, M. J. Flexible Mesoporous Photonic Resins with Tunable Chiral Nematic Structures. *Angew. Chem., Int. Ed.* **2013**, *52*, 8921–8924.
- (59) Nguyen, T.-D.; Hamad, W. Y.; MacLachlan, M. J. CdS Quantum Dots Encapsulated in Chiral Nematic Mesoporous Silica: New Iridescent and Luminescent Materials. *Adv. Funct. Mater.* **2014**, *24*, 777–783.